Synthesis of Comblike Poly(butyl methacrylate) Using Reversible Addition−Fragmentation Chain Transfer and an Activated Ester

Johannes J. Vosloo,[†,‡] Matthew P. Tonge,[‡] Christopher M. Fellows,[†] Franck D'Agosto,[§] Ronald D. Sanderson,[‡] and Robert G. Gilbert*[,†]

Key Centre for Polymer Colloids, School of Chemistry F11, University of Sydney, NSW 2006, Australia; UNESCO Associated Centre for Macromolecules and Materials, Department of Chemistry and Polymer Science, University of Stellenbosch, Private Bag X1, De Beers Street, Matieland, 7602, South Africa; and LCPP CPE/CNRS, Bât 308 F, 43 Blvd du 11 Novembre 1918, BP 2077, 69616 Villeurbanne Cedex, France

Received September 4, 2003; Revised Manuscript Received January 22, 2004

ABSTRACT: Comblike polymers of poly(*n*-butyl methacrylate) were prepared using an activated ester-type comonomer (*N*-acryloxysuccinimide, NAS) to generate branch points. The conventional solution free-radical copolymerization kinetics of *n*-butyl methacrylate (BMA) and NAS were first investigated by following individual monomer consumption rates by ^{1}H NMR spectrometry and reactivity ratios of BMA and NAS determined using the terminal model. The reactivity ratios so obtained are both close to 0.2; the joint confidence interval is also determined. Reversible addition−fragmentation chain transfer (RAFT) was then used to grow polymers with controlled backbone and branch chain length. Because both reactivity ratios have similar values, this implies that the copolymer will have a random distribution of NAS and hence of branch points. RAFT-mediated polymerization was first used to synthesize linear poly(BMA-*co*-NAS) chains. Primary hydroxy-functionalized RAFT agents were then immobilized on this linear poly(BMA-*co*-NAS) through nucleophilic substitution on the activated ester units of the NAS. From these immobilized RAFT agents, branches were grown upon addition of a further aliquot of monomer (BMA) and initiator (AIBN). The amount of NAS in the starting BMA/NAS composition was varied without adversely affecting the uniformity of the NAS distribution along the resulting linear poly(BMA-*co*-NAS) backbone. This results in branched polymers whose molecular weight, branching density, and degree of polymerization of branches are all relatively narrow and controlled.

Introduction

Gaining control over polymer architecture is an alluring prospect since it enables control over resulting material properties. Control at a molecular level would enable the synthesis of polymers made up of the same chemical repeat unit, yet potentially with different mechanical properties with a wide range of possible applications. Different architectures and microstructures include linear chains, various copolymers (e.g., gradient, alternating, and random), block copolymers (AB, ABA, etc.), stars, dendrites, combs, and pom-poms.

Molecular architectures related to branched structures and the resulting mechanical properties have generated considerable interest.[1−5] Creating a palette of polymers with (say) identical chemical composition and backbone chain length, but where branching density and branch molecular weight can be systematically varied, opens the way to test theories of these mechanical properties.

Various polymerization techniques can be used to prepare branched structures, including polycondensation,[6,7] ionic polymerization,[8−10] and free radical polymerization.[11] While condensation polymerization reactions are relatively simple, ionic techniques require very stringent reaction conditions. Alternatively, the industrial importance and robustness of free radical polymerization, relatively mild reaction conditions and the continued improvement of various controlled free radical polymerization techniques, make the free radical route an appealing option. Reversible addition−fragmentation chain transfer (RAFT),[12] atom transfer radical polymerization (ATRP),[13] and nitroxide-mediated radical polymerization (NMP)[14] offer simple and efficient routes to polymers of comblike structure.

Apart from the polymerization technique used, there exist three general approaches to synthesizing polymers that exhibit branched architectures.

The first approach (Scheme 1a) comprises the synthesis of macromonomers. Some of the approaches used to synthesize macromonomers include the catalytic chain transfer (CCT) technique,[15−17] conventional organic routes,[18,19] addition−fragmentation reaction techniques,[20] conventional chain transfer to polymer,[21] and ATRP.[22−25] All of these techniques yield low molecular weight oligomers with terminal vinyl end groups or other terminal functional end groups capable of being polymerized. These macromonomers can subsequently be copolymerized with other monomers in various ratios to yield branched polymers.[22,26−28] Macromonomers are most useful when very short branches are required.

The second approach (Scheme 1b) involves the synthesis of a linear polymer containing functional monomer(s) distributed along the polymer chain. In a separate step, polymers that have been end-functionalized are prepared. These end-functionalized polymers are subsequently reacted covalently with the functional groups distributed along the original polymer backbone.[10,29−32] This approach allows the chains that eventually serve as branches to be characterized extensively before incorporation into the backbone and is often called the "grafting onto" approach.

† University of Sydney.
‡ University of Stellenbosch.
§ LCPP CPE/CNRS.
* Corresponding author: Fax +61-2-9351 8651, e-mail gilbert@chem.usyd.edu.au.

10.1021/ma035302a CCC: $27.50 © 2004 American Chemical Society
Published on Web 03/04/2004

Scheme 1. Different Approaches for Synthesizing Polymers with Controlled Branched Structures: (a) Use of Macromonomers, (b) "Grafting Onto" Approach, and (c) "Grafting From" Approach; M = Monomer, A, X, Y and I = Appropriate Functional Groups

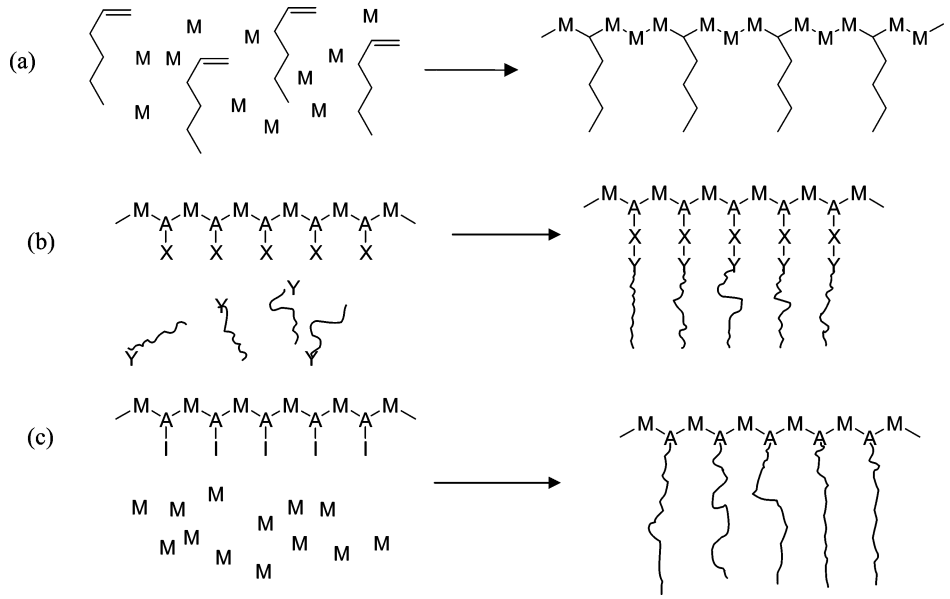

Scheme 2. Structures of *N*-Acryloxysuccinimide (NAS) (1), *n*-Butyl Methacrylate (BMA) (2), 2-{[(Dodecylsulfanyl)carbonothioyl]sulfanyl}-propanoic Acid (3), Benzyl 2-(2-Hydroxyethylamino)-1-methyl-2-oxoethyl Trithiocarbonate (4), 2-Phenylpropyl Phenyldithioacetate (5), and 2-Cyanopropyl Dithiobenzoate (6)

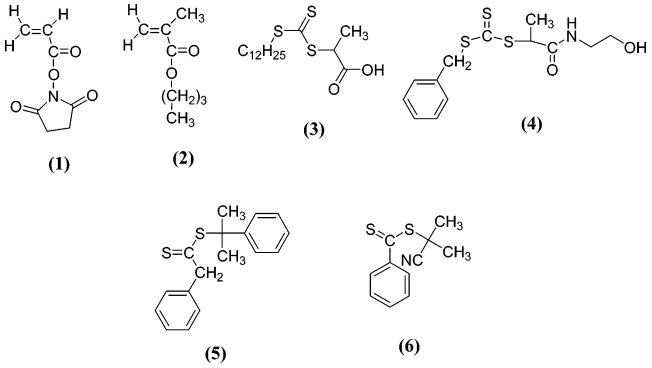

The third approach (Scheme 1c) also requires the synthesis of a linear polymer backbone incorporating a functional monomer. The functional monomer must contain a chemical group which either directly or after chemical modification is capable of participating in initiating a polymerization reaction. These functional monomers act as sites from which branches can grow upon addition of monomer (and an appropriate initiator, if required).[19,33−36] In some cases the formed branches can be chemically cleaved from the backbone and characterized.[37] This approach is often referred to as the "grafting from" approach.

In this study the "grafting from" approach was employed. *n*-Butyl methacrylate (BMA **(2)**, Scheme 2) was the main monomer, and *N*-acryloxysuccinimide (NAS (**1**), Scheme 2) was selected as the functional monomer to be incorporated into the poly(BMA) backbone. NAS is an activated ester-type monomer:[38−43] the presence of the electron-withdrawing succinimide moiety renders the carbonyl carbon of the ester susceptible to nucleophilic substitution reactions. NAS has been employed as a functional monomer in various copolymers to impart a range of desired properties and capabilities.[44−52]

To ensure a truly random distribution of branches along a poly(BMA-*co*-NAS-*graft*-BMA) molecule, a random distribution of potential branch points must be present in the "parent" chain. To achieve this, the free radical copolymerization kinetics of BMA and NAS were investigated and reactivity ratios for the BMA- and NAS-terminated polymer radicals determined, assuming the terminal model.[53−55] The data so obtained permit conditions to be chosen so as to maintain a constant copolymer composition throughout the course of a polymerization and thus a random distribution along a poly(BMA-*co*-NAS) chain throughout the course of a reaction. The incorporation of BMA and NAS into a propagating chain was investigated by monitoring changes in individual free monomer concentrations by ^{1}H NMR spectrometry.

As controlled radical techniques do not significantly affect reactivity ratios when compared to conventional free radical systems,[56−58] RAFT was employed to control backbone length. RAFT-mediated copolymerization of BMA and NAS in the feed region of interest was investigated. The presently accepted mechanism for the RAFT process is as follows.[12] Initiator-derived primary radicals react with monomer units to form oligomeric radicals, which undergo addition to the carbon−sulfur double bond of the dithioester chain transfer agents. The resulting radical then loses a good homolytic leaving group, as a radical capable of either initiating a polymerization reaction or, in the case of a polymeric leaving species, propagating further. Equilibrium is established between active (propagating) and dormant polymer chains via the subsequent addition and fragmentation steps. The RAFT mechanism has been discussed in detail elsewhere.[12,59,60]

Experimental Section

Chemicals. *N*-Hydroxysuccinimide (NHS, Aldrich, 97%), acryloyl chloride (Aldrich, 96%), triethylamine (Et_3N, Aldrich, 99.5%), 4-(dimethylamino)pyridine (DMAP, Aldrich, 99+%), and 1,3,5-trioxane (Fluka AG, 97%) were used as received. 1,4-Dioxane was distilled over $LiAlH_4$ to remove any traces of

Scheme 3. Synthesis of *N*-Acryloxysuccinimide (NAS)

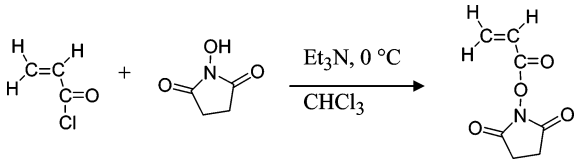

water and other impurities. Chloroform was distilled prior to use. Butyl methacrylate (BMA, Aldrich, 99%) was extracted with two equal aliquots of a 0.3 M aqueous KOH solution to remove inhibitors and distilled at reduced pressure. The middle fraction was collected and stored over molecular sieves (4 Å) at 2 °C for later use. Azobis(isobutyronitrile) (AIBN, Delta Scientific, 98%) was recrystallized from methanol. The water was distilled and deionized (DDI).

The following RAFT agents were used. 2-{[(Dodecylsulfanyl)-carbonothioyl]sulfanyl}propanoic acid (**3**): The synthesis of this RAFT agent is described elsewhere.[61] Benzyl 2-(2-hydroxyethylamino)-1-methyl-2-oxoethyl trithiocarbonate (**4**): This RAFT agent was supplied by the Key Centre for Polymer Colloids with the permission of Dulux, Australia. The synthetic procedure will be disclosed in a forthcoming patent. Benzyl 2-(2-hydroxyethylamino)-1-methyl-2-oxoethyl trithiocarbonate (**4**) was selected for immobilization on the poly(BMA-*co*-NAS) backbone since the compound contained a primary hydroxy functionality needed for nucleophilic substitution reactions with NAS units.

NAS Synthesis. NAS was synthesized by reacting acryloyl chloride (11.71 g, 1.29×10^{-1} mol) and *N*-hydroxysuccinimide (NHS, 15.15 g, 1.32×10^{-1} mol) in the presence of triethylamine (14.40 g, 1.42×10^{-1} mol) at 0 °C in $CHCl_3$ (200 mL), as shown in Scheme 3. Details of the synthesis and purification procedures have been reported elsewhere.[44] ^{1}H NMR was used to verify that the product was free of any side products as described in detail by d'Agosto et al.[62] The final yield was 57%.

NMR Spectrometry Analysis. ^{1}H NMR spectra were recorded on a Bruker AVANCE DPX300 spectrometer. The instrument frequency was 300 MHz with the default number of scans being eight. $CDCl_3$ and 1,4-dioxane-d_8 were used as solvents. TMS was used as internal reference. Accurate high-temperature calibration was done using an ethylene glycol sample.[63]

Determination of Reactivity Ratios. BMA/NAS copolymerization reactions were conducted in 1,4-dioxane at 60 °C using AIBN as initiator. The reaction mixture was purged with N_2 for 30 min before heating the mixture to the reaction temperature. Samples were removed and individual monomer concentrations followed using ^{1}H NMR spectrometry. Monomer concentrations were calibrated by comparing the signals of the vinylic protons corresponding to the different monomers with that of an inert internal reference, 1,3,5-trioxane.[44] For each different BMA/NAS starting composition, a ^{1}H NMR spectrum of the entire reaction mixture was recorded before the start of the reaction and after running the reaction for 30 min. The ratio of the integrated signals of the vinylic protons for each monomer to the integrated signal of the internal reference, before and after reaction, was used to calculate the individual monomer consumption during the course of the copolymerization reaction.

Reactivity ratios were determined applying a least-squares nonlinear fitting procedure to eq 1 using code developed and discussed by van Herk.[64] Further refining of the reactivity ratios was done using the Tidwell−Mortimer method.[65] The 95% confidence interval was also obtained using van Herk's code.[64] In situ ^{1}H NMR spectrometry data were obtained by conducting a BMA/NAS copolymerization reaction starting from a ∼50/50 (BMA/NAS) ratio in the NMR instrument. A reaction mixture containing BMA (0.069 g, 4.8×10^{-4} mol), NAS (0.076 g, 4.5×10^{-4} mol), AIBN (0.007 g, 4.3×10^{-5} mol), 1,3,5-trioxane (0.013 g, 1.5×10^{-4} mol), and 1,4-dioxane (3.0 mL) was prepared and degassed by purging with N_2 for 30 min. Ca. 800 μL of this mixture was transferred to an NMR spectrometer tube containing 3 drops of 1,4-dioxane-d_8 and degassed in the same manner for an additional 10 min. The sample cavity of the NMR instrument was heated to 60 °C (after accurate temperature calibration), and the sample was lowered into the cavity. Instantaneous individual monomer concentrations were measured every 3 min using a single scan only, employing the technique described earlier.

Molecular Weight Analyses. Molecular weights were determined using size exclusion chromatography (SEC). Samples were prepared for SEC analysis by drying the polymer in vacuo and redissolving ca. 5 mg of the polymer in 1 mL of THF. The SEC instrument consisted of a Waters 717_{plus} autosampler, a Waters 600E system controller, and a Waters 610 fluid unit. A Waters 410 differential refractometer was used at 35 °C as detector. Tetrahydrofuran (THF, HPLC-grade) sparged with IR-grade helium was used as eluent at a flow rate of 1 mL min^{-1} and 60 min per sample. The column oven was kept at 35 °C, and the injection volume was 100 μL. Four Phenogel columns (300 mm × 7.80 mm) with respective pore sizes of 100, 10^3, 10^4, and 10^5 Å were used in series. The system was calibrated using six narrow polystyrene molecular weight standards in the range 4000−2000 000, supplied by Pressure Chemical. All molecular weights were calculated relative to polystyrene.[61]

Poly(BMA-*co*-NAS) Synthesis. NAS content was varied. A typical reaction mixture contained BMA (5.028 g, 3.511×10^{-2} mol), NAS (1.190 g, 7.036×10^{-3} mol), AIBN (0.007 g, 4.3×10^{-5} mol), 2-{[(dodecylsulfanyl)carbonothioyl]sulfanyl}-propanoic acid (**3**, 0.072 g, 2.1×10^{-4} mol), 1,3,5-trioxane (0.082 g, 9.1×10^{-4} mol), and 1,4-dioxane (22.0 mL). The reaction mixture was purged with N_2 for 30 min before heating to the reaction temperature of 80 °C. Individual monomer conversions were determined by withdrawing samples at regular intervals for analysis by ^{1}H NMR spectrometry as described earlier, without any precipitation or purification. The final resulting polymer was precipitated in an excess amount of cyclohexane and/or hexane, washed, and dried in vacuo. Methanol was not used for precipitation of the resulting polymer to prevent any substitution reactions of methanol with the activated ester units. The final yield for the example above was 90%.

Immobilization of RAFT Agent onto Poly(BMA-*co*-NAS). Benzyl 2-(2-hydroxyethylamino)-1-methyl-2-oxoethyl trithiocarbonate (**4**) was immobilized on the poly(BMA-*co*-NAS) backbone by refluxing in $CHCl_3$ for 48 h in the presence of a catalytic amount of 4-(dimethylamino)pyridine (DMAP) (Scheme 4). The resulting polymer was precipitated in an excess amount of methanol, after which the sample was filtered and washed with additional methanol to remove formed byproducts. The sample was redissolved in chloroform, and the filtering and washing procedure was repeated. The material was dried in vacuo to remove residual solvent. The immobilization yield was determined by monitoring the decrease of the succinimide-CH_2 signal (4 H at ca. δ = 2.80 ppm, $CDCl_3$) in the ^{1}H NMR spectrum, using a methylene group in the BMA alkyl-ester chain (2 H at ca. δ = 3.95 ppm, $CDCl_3$) as an internal reference. A typical reaction mixture contained poly(BMA-*co*-NAS) (2.00 g, ca. 20% NAS), benzyl 2-(2-hydroxyethylamino)-1-methyl-2-oxoethyl trithiocarbonate (**4**, 1.183 g, 3.750×10^{-3} mol), DMAP (0.034 g, 2.8×10^{-4} mol), and $CHCl_3$ (50.0 mL). The final immobilization yield for this example was 83%.

Synthesis of Poly(BMA-*co*-NAS-*graft*-BMA). Poly(BMA-*co*-NAS) with immobilized RAFT agent (**4**) on the NAS units was dissolved in $CHCl_3$. AIBN was used as free radical initiator (Scheme 4) in the molar ratio [immobilized RAFT agent]:[AIBN] = 10:1. BMA was used as monomer for the branches in a stoichiometric quantity that targeted a branch molar mass of ∼6000. The reaction mixture was purged with N_2 for 30 min before heating to the reaction temperature of 60 °C. The resulting polymer was precipitated in an excess amount of methanol and conversion was determined gravimetrically. A typical reaction mixture contained poly(BMA-*co*-NAS-*graft*-RAFT agent) (1.365 g, i.e., containing ca. 20% immobilized RAFT agent), BMA (9.691 g, 6.767×10^{-2} mol), AIBN (0.026 g, 1.6×10^{-4} mol), and $CHCl_3$ (40.0 mL). The final yield for this example was 77%.

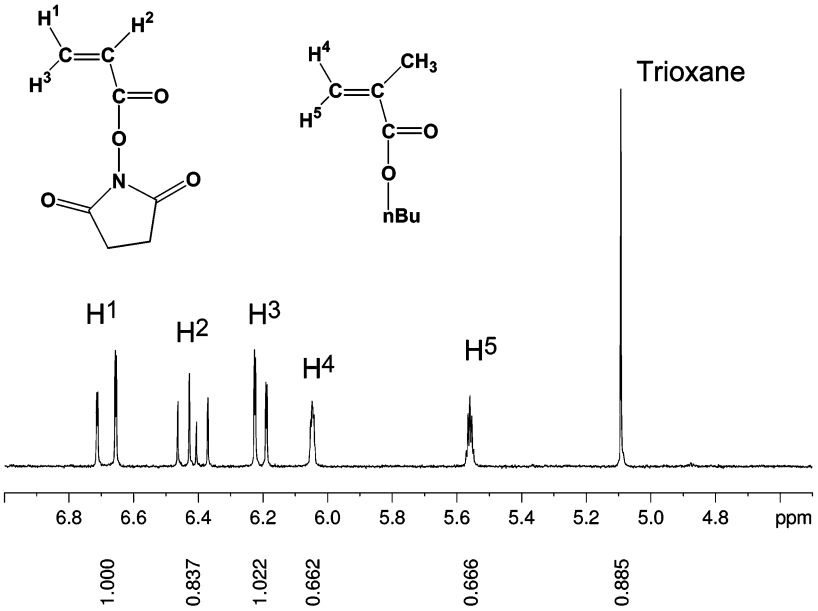

Figure 1. ^{1}H NMR spectrum ($CDCl_3$) of a BMA/NAS (40/60) copolymerization reaction mixture showing the region of interest. The spectrum shows the signals corresponding to the vinylic protons of the two respective monomers relative to 1,3,5-trioxane.

Scheme 4. Immobilization of Primary Hydroxy-Functionalized RAFT Agents (Benzyl 2-(2-Hydroxyethylamino)-1-methyl-2-oxoethyl Trithiocarbonate (4)) on a Poly(BMA-*co*-NAS) Backbone and Subsequent Branch Synthesis

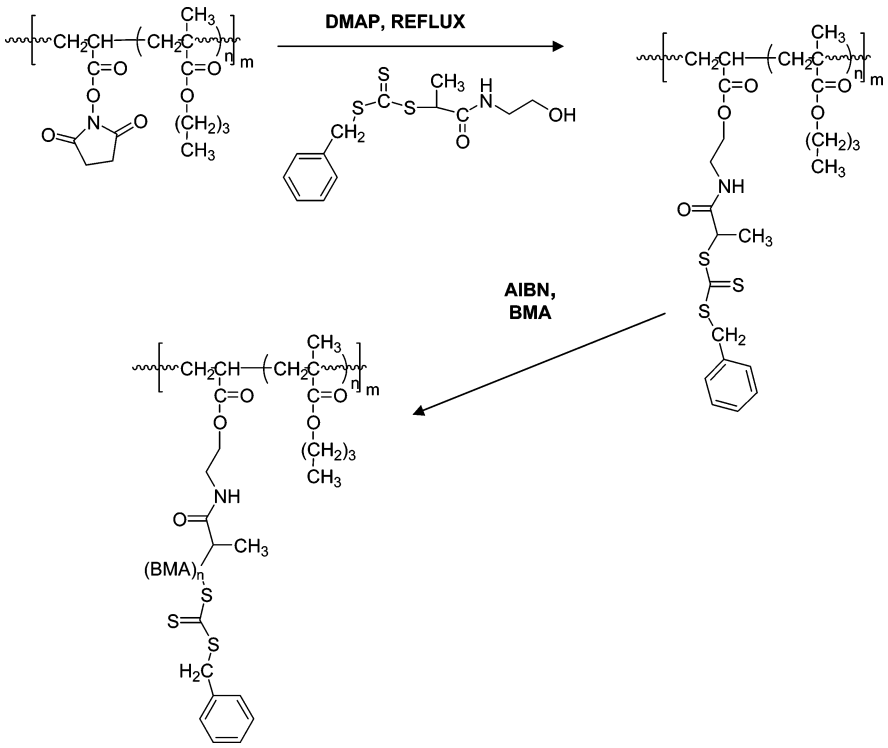

Results and Discussion

BMA/NAS Copolymerization Kinetics. In this study individual monomer conversions were determined by ^{1}H NMR spectrometry before reaction and after stopping conventional free radical BMA/NAS copolymerization reactions at low conversions for a number of different BMA/NAS starting compositions. Nonlinear (least-squares) fitting to eq 1 was used to determine the reactivity ratios:[66,67]

$$F_1 = \frac{r_1 f_1^{\,2} + f_1 f_2}{r_1 f_1^{\,2} + 2 f_1 f_2 + r_2 f_2^{\,2}} \qquad (1)$$

where F_1 is the fraction of monomer M_1 in the copolymer, f_1 and $f_2 = 1 - f_1$ the fractions of monomer M_1 and monomer M_2 in the feed, respectively, and r_1 and r_2 the reactivity ratios.

^{1}H NMR analysis (as described earlier) enabled the determination of F_{BMA} and f_{BMA} values. An example of a ^{1}H NMR spectrum for a typical BMA/NAS copolymerization reaction mixture is shown in Figure 1. It was assumed that all monomer not present in the reaction mixture as free monomer had been incorporated into the polymer chain. F_{NAS} and f_{NAS} values were obtained in the same manner. The reactivity ratios obtained by least-squares fitting to eq 1 were $r_{BMA} = 0.98$ (+0.51,

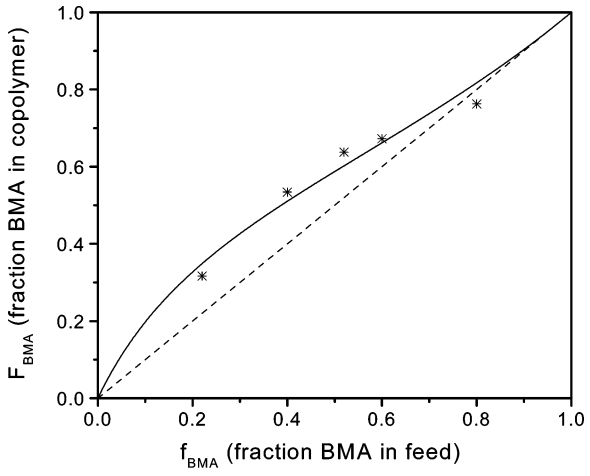

(a)

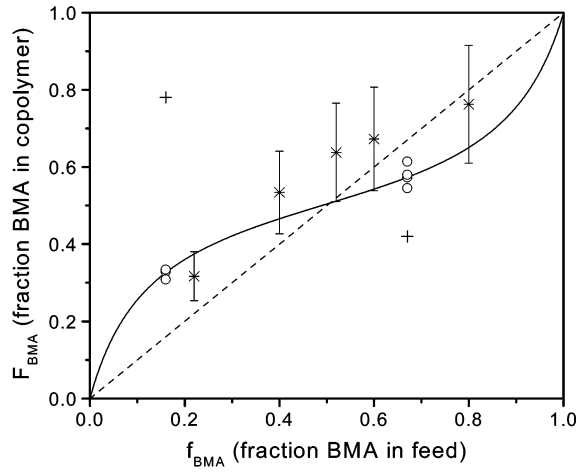

(b)

Figure 2. Copolymer composition vs feed composition for the conventional free radical copolymerization of BMA and NAS conducted in 1,4-dioxane at 60 °C using AIBN as initiator (a) using the initial estimates for the reactivity ratios and (b) after refinement of the reactivity ratios using the Tidwell−Mortimer approach. The diagrams show the azeotrope (dashed) and the experimentally obtained data points (∗, for initial estimate; ○, for Tidwell−Mortimer experiments; +, for outliers in the Tidwell−Mortimer series) to which the fitting (solid) was done.

−0.36) and r_{NAS} = 0.39 (+0.57, −0.17). The compositional diagram constructed using the reactivity ratios so calculated is shown as Figure 2a. These values in turn served as the good estimate needed to employ the Tidwell−Mortimer method,[65] which uses a good first estimation of a set of reactivity ratios to predict the two feed compositions at which the errors are at a minimum. This leads to a set of reactivity ratios having the smallest possible confidence interval. A number of experiments are consequently conducted at each of these compositions. The two feed compositions were determined using the following expressions:

$$f'_{BMA} \approx \frac{2}{2 + r_{BMA}} \quad \text{and} \quad f''_{BMA} \approx \frac{r_{NAS}}{2 + r_{NAS}}$$

The two optimum feed compositions were calculated to be $f'_{BMA} = 0.67$ and $f''_{BMA} = 0.16$. Experiments done at these feed compositions were done exactly as those described earlier; results are shown in Table 1. The reactivity ratios obtained from these data were r_{BMA} =

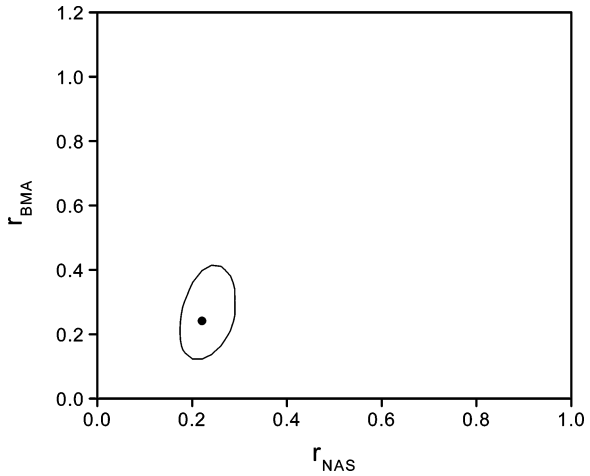

Figure 3. 95% confidence interval associated with the obtained final values for the reactivity ratios for the copolymerization of BMA and NAS in 1,4-dioxane at 60 °C using AIBN as initiator.

0.241 (+0.089, −0.060) and r_{NAS} = 0.221 (+0.037, −0.024). These reactivity ratios enabled the construction of a compositional diagram as shown in Figure 2b. Error bars on the initial data points were calculated by assuming a 5% uncertainty in integration values obtained from ^{1}H NMR spectra and calculating the total uncertainty as the sum of these individual uncertainties. Although a slight compositional drift can be seen in Figure 2b, the copolymer composition remains relatively close to the azeotrope. Figure 2 illustrates the care that should be taken when using data points obtained from a single experimental run. Figure 2b shows discarded outliers observed at each of the two optimum feed compositions which could have been taken as valid data points, had repeated runs not been done. Repeated runs at identical feed compositions (as was done in Figure 2b) ensured that eventual data points were trustworthy. The 95% confidence interval associated with the final values of the reactivity ratios is shown in Figure 3. The behavior predicted by the compositional diagram in Figure 2b is supported by the data in Figure 4, which show the decrease in individual monomer concentrations of BMA and NAS for an approximately equimolar starting ratio. The individual BMA and NAS concentrations decreased at similar rates. This was expected since an equimolar feed composition lies very close to the predicted azeotrope. Starved-feed protocols were considered unnecessary to ensure a uniform distribution of NAS units along the poly(BMA-*co*-NAS) backbone, since copolymer composition remained in the vicinity of the azeotrope through the feed range.

Poly(BMA-*co*-NAS) Synthesis. RAFT was used to control backbone poly(BMA-*co*-NAS) synthesis. Figures 5−8 show conversion data as functions of time for the solution RAFT copolymerization of BMA and NAS starting from different (BMA/NAS) molar ratios for different [AIBN]:[RAFT agent] ratios. These data comprise individual monomer conversions as obtained using ^{1}H NMR spectrometry, and $\ln([M]_0/[M]_t)$, where $[M]_t$ = monomer concentration at time t. If ideal free radical kinetics were obeyed, $\ln([M]_0/[M]_t)$ would be linear in t. It is clear from the data in Figures 5 and 7 that both monomers were consumed at a comparable rate (with respect to relative individual starting concentrations) throughout the course of the copolymerization reaction. A slight preference was shown toward NAS, as predicted

Table 1. ^{1}H NMR Spectrometry Results for BMA/NAS Copolymerization Reactions[a]

reaction ID	composition (BMA/NAS)	I(NAS)[b] at t = 0 min	I(NAS)[b] at t = 30 min	$[NAS]_0$[c] (M)	$[NAS]_t$[d] (M)	I(BMA)[e] at t = 0 min
1	16/84	0.967	0.945	0.252	0.211	0.222
2	16/84	0.967	0.941	0.252	0.202	0.222
3	16/84	0.967	0.947	0.252	0.198	0.222
4	67/33	0.982	0.961	0.099	0.087	1.897
5	67/33	0.982	0.969	0.099	0.091	1.897
6	67/33	0.982	1.007	0.099	0.077	1.897
7	67/33	0.982	0.960	0.099	0.087	1.897

reaction ID	I(BMA)[e] at t = 30 min	$[BMA]_0$[f] (M)	$[BMA]_t$[g] (M)	I(trioxane)[h] at t = 0 min	I(trioxane)[h] at t = 30 min	FBMA[i]	FNAS[i]
1	0.152	0.049	0.029	0.242	0.283	0.33	0.67
2	0.131	0.049	0.024	0.242	0.294	0.33	0.67
3	0.141	0.049	0.025	0.242	0.301	0.31	0.69
4	1.945	0.201	0.184	1.054	1.178	0.57	0.43
5	1.937	0.201	0.191	1.054	1.128	0.55	0.45
6	2.066	0.201	0.165	1.054	1.394	0.61	0.39
7	1.938	0.201	0.184	1.054	1.175	0.58	0.42

[a] All reactions were done in 1,4-dioxane at 60 °C using AIBN as initiator. For all reactions: [BMA + NAS] = 0.3 M, [AIBN]/[monomer] = 0.005. [b] Normalized integrals of vinylic protons of NAS. [c] Initial monomer concentration. [d] Final monomer concentration. [e] Normalized integrals of vinylic protons of BMA. [f] Initial monomer concentration. [g] Final monomer concentration. [h] Normalized integrals of vinylic protons of trioxane. [i] Copolymer composition.

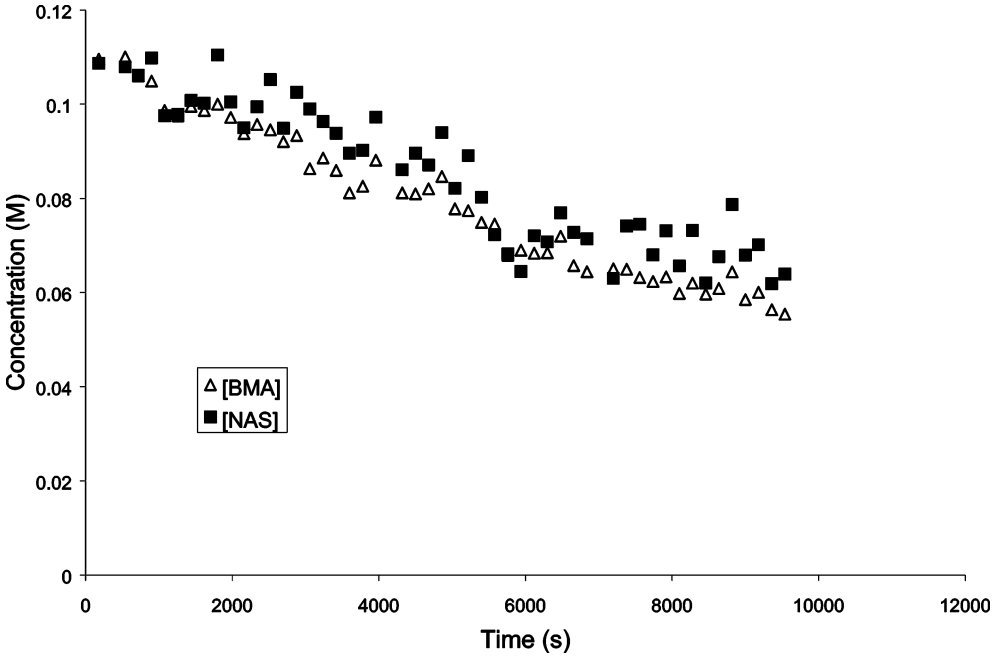

Figure 4. Monomer concentration (M) vs time (s) for the conventional free radical solution copolymerization of BMA and NAS (50/50) in 1,4-dioxane at 60 °C, as obtained using in situ ^{1}H NMR spectrometry measurements.

by the reactivity ratios. Theoretical composition values were well within range of observed composition values, as determined using free monomer concentrations. Now, the reactivity ratios were determined at 60 °C compared to 80 °C for the rate data shown in these figures. The effect of temperature on reactivity ratios, as described elsewhere, is to increase the randomness of incorporation; i.e., reactivity ratios approach 1 as the reaction temperature increases.[68] Since the reactivity ratios do not differ by a significant amount, no detrimental impact on the uniformity of the NAS distribution is expected. The polymerization reaction proceeded rapidly, as expected of systems employing trithio-type RAFT agents.[69,70] Figures 5 and 7 also show the decrease in consumption rates as the ratio of AIBN to RAFT agent was changed from 1:5 to 1:10 by decreasing the amount of AIBN. This change is the expected result of a lower propagating radical concentration. The relative incorporation rates of BMA and NAS, however, remained largely unchanged with changing initiator concentration.

Figures 6 and 8 illustrate the relationship between reaction rate for the individual monomers and reaction time for different initiator concentrations (while maintaining a constant RAFT agent concentration) in the RAFT solution copolymerization of BMA and NAS for different BMA/NAS starting compositions. No evidence to suggest significant autoacceleration at higher conversion was observed, although a slight decrease in reaction rate with increasing conversion can be seen for the 90/10 (BMA/NAS) starting composition. The consumption rates for both BMA and NAS also indicate that the incorporation of both monomers proceeded in an even and controlled manner, with the expected minor preference toward NAS. Even at relatively extreme feed compositions such as 80/20 and 90/10 (BMA/NAS), no

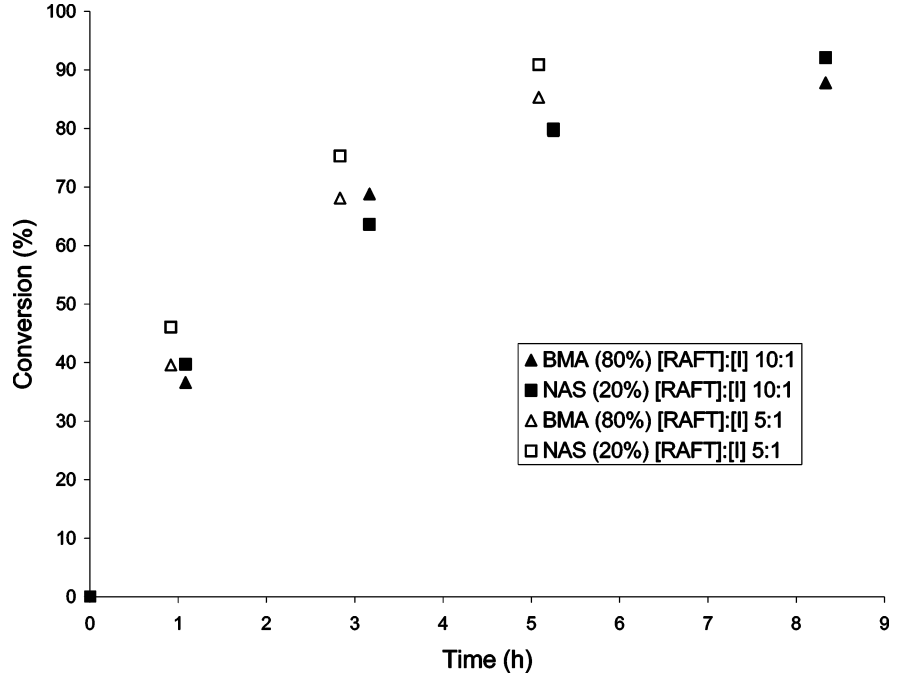

Figure 5. Monomer conversion vs time for the RAFT solution BMA/NAS (80/20) copolymerization reaction for different [RAFT agent]:[AIBN] ratios conducted in 1,4-dioxane at 80 °C.

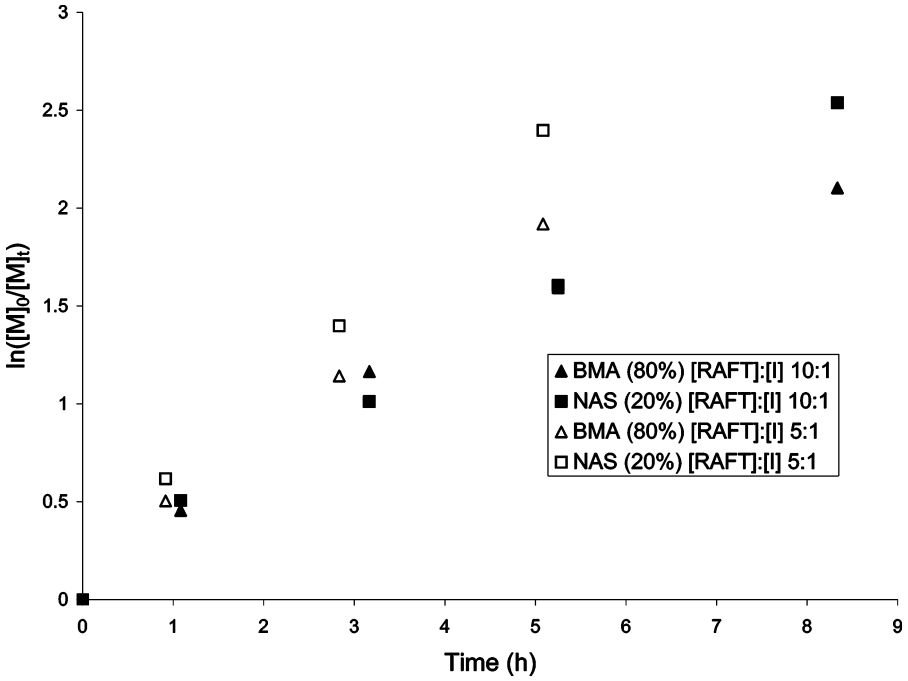

Figure 6. $\ln([M]_0/[M]_t)$ vs time for the RAFT solution BMA/NAS (80/20) copolymerization for different [RAFT agent]:[AIBN] ratios conducted in 1,4-dioxane at 80 °C.

significant drift in relative consumption rates was observed. This observation suggests a relatively random distribution of NAS units along the backbone, which is critical for a random distribution of branches in the target comblike molecules.

Molecular weight distributions of poly(BMA-*co*-NAS) showed a degree of tailing toward the low molecular weight end, as can be seen in Figure 9. Increasing low molecular weight tailing corresponding to an increasing NAS content observed during the SEC of poly(BMA-*co*-NAS) can also be seen in Figure 9. A possible explanation is the formation of low molecular weight species due to termination events occurring early during the RAFT process. This type of tailing was also observed in the synthesis of BMA homopolymer throughout the course of the polymerization reaction. The low molecular weight tail gave rise to higher than expected polydispersities ($1.5 < \bar{M}_w/\bar{M}_n$). The data presented in Figure 10 show the molecular weight distributions of poly(BMA-*co*-NAS) prepared under identical conditions, apart from the type of RAFT agent used. Moving through the different families of RAFT agents—from the RAFT agent giving the fastest reaction rate to the RAFT agent giving the slowest reaction rate in going from **3** to **5** to **6** (Scheme 2)—the troublesome low molecular weight tailing decreases. This suggests that this specific system might be sensitive toward termination events occurring or lack of efficiency either during the initial

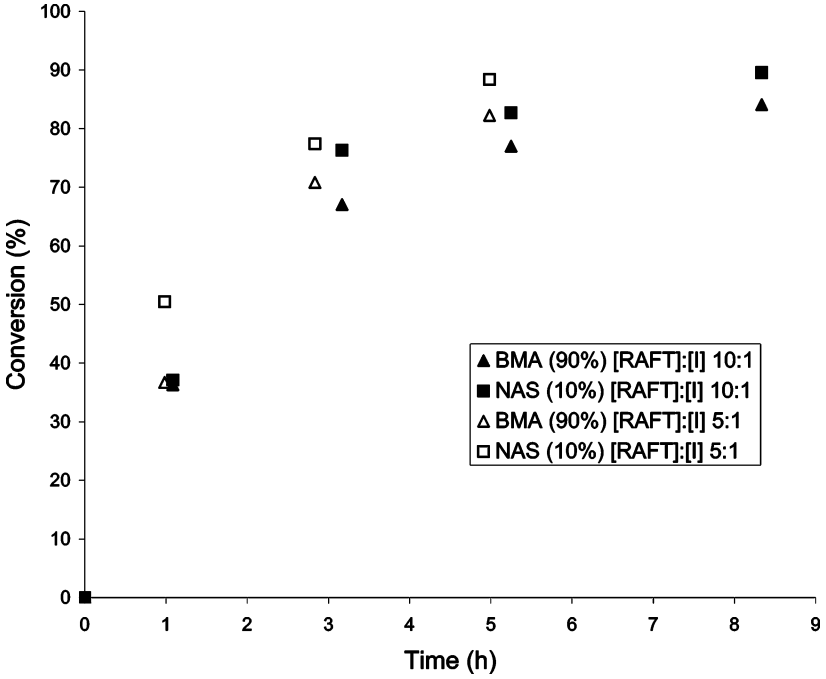

Figure 7. Monomer conversion vs time for the RAFT solution BMA/NAS (90/10) copolymerization reaction for different [RAFT agent]:[AIBN] ratios conducted in 1,4-dioxane at 80 °C.

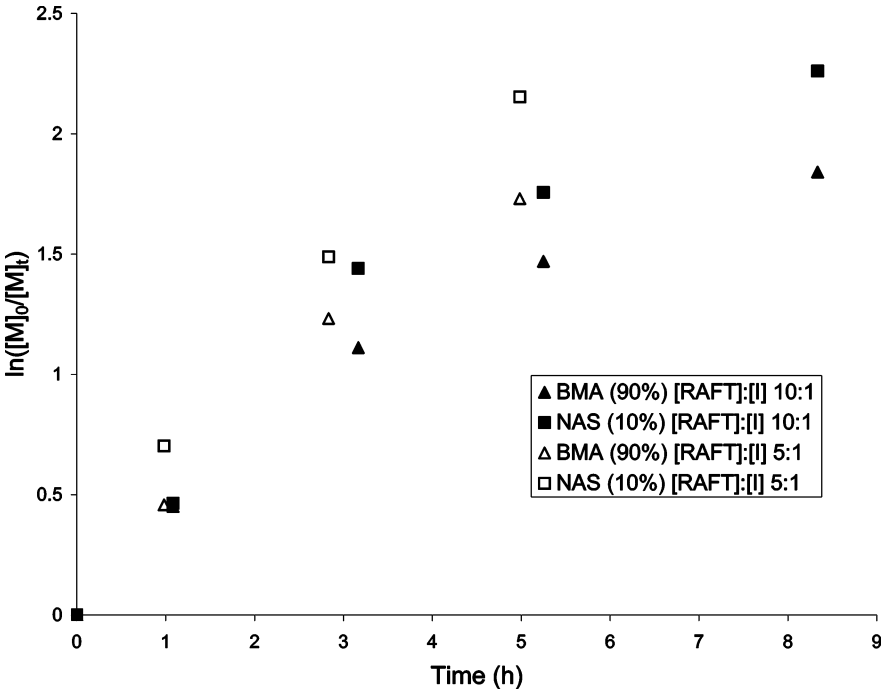

Figure 8. $\ln([M]_0/[M]_t)$ vs time for the RAFT solution BMA/NAS (90/10) copolymerization for different [RAFT agent]:[AIBN] ratios conducted in 1,4-dioxane at 80 °C.

preequilibrium in the RAFT process or during normal chain propagation throughout the polymerization reaction.

Immobilization of RAFT Agents on Poly(BMA-*co*-NAS). Once a desired NAS distribution and content were obtained, primary hydroxy-functionalized RAFT agents (benzyl 2-(2-hydroxyethylamino)-1-methyl-2-oxoethyl trithiocarbonate (**4**), Scheme 2) were reacted with the polymer. The reaction was catalyzed using 4-(dimethylamino)pyridine (DMAP). The immobilization yield of benzyl 2-(2-hydroxyethylamino)-1-methyl-2-oxoethyl trithiocarbonate (**4**) onto NAS units in the poly(BMA-*co*-NAS) backbone was determined by monitoring the decrease in intensity of the succinimide-CH_2 signal from the NAS units (4 H at ca. $\delta = 2.80$ ppm, $CDCl_3$) in the ^{1}H NMR spectrum, relative to a methylene group signal from the BMA alkyl-ester chain (2 H at ca. $\delta = 3.95$ ppm, $CDCl_3$) as an internal reference (Figure 11). The intensity of the succinimide-CH_2 signal decreased relative to the intensity of the alkyl-ester methylene signal, indicating that reaction between **4** and the succinimide moiety (resulting in substitution of the succinimide group) took place through the course of the substitution reaction. Integration of the benzyl peak (5 H at ca. $\delta = 7.4$ ppm, $CDCl_3$) and subsequent comparison with the alkyl-ester reference signal, as an alternative to obtain

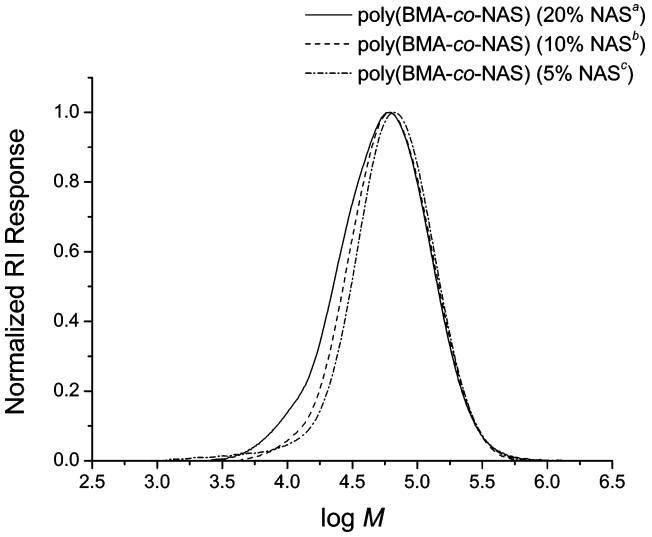

Figure 9. Molecular weight distributions of poly(BMA-*co*-NAS) containing different amounts of NAS prepared using RAFT agent (**3**): (a) $\bar{M}_n = 35\,600$, PDI = 1.98; (b) $\bar{M}_n = 45\,200$, PDI = 1.67; (c) $\bar{M}_n = 45\,600$, PDI = 1.75.

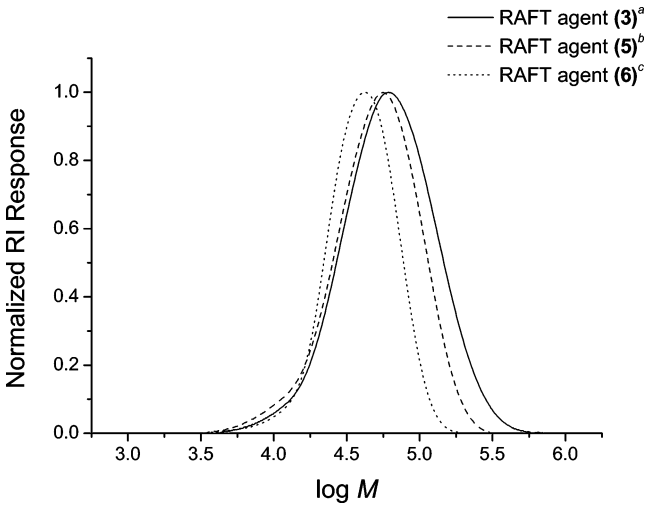

Figure 10. Molecular weight distributions of poly(BMA-*co*-NAS) containing 10% NAS prepared using different RAFT agents: (a) $\bar{M}_n = 45\,200$, PDI = 1.67; (b) $\bar{M}_n = 38\,300$, PDI = 1.56; (c) $\bar{M}_n = 26\,300$, PDI = 1.64.

immobilization yield, showed excellent agreement with the result obtained from following the decrease in intensity of the succinimide-CH_2 signal. Immobilization of **4** became progressively more difficult with decreasing NAS content in the poly(BMA-*co*-NAS). Poly(BMA-*co*-NAS) containing 20% NAS was reacted to ~90% grafting efficiency in less than 24 h, but poly(BMA-*co*-NAS) containing 10% and 5% NAS respectively appeared to reach a ceiling grafting yield of 50−60%. Residual, unreacted NAS units in the polymer backbone should not have any detrimental effect on the behavior of the resulting polymers when subjected to the subsequent free radical polymerization steps. The activated-ester moiety only undergoes substitution-type reactions and is therefore not expected to react with primary free radicals originating from AIBN or other propagating radicals. The presence of the immobilized RAFT agents on the poly(BMA-*co*-NAS) backbone rendered the material only partially soluble in THF, making accurate SEC analysis of the poly(BMA-*co*-NAS-*graft*-RAFT agent) impossible. It is, however, expected that immobilized RAFT agents added as pendant side groups to a linear chain would not impact greatly on the molecular weight distribution of the poly(BMA-*co*-NAS) as determined prior to RAFT agent immobilization. The molecular weight distribution of poly(BMA-*co*-NAS) was considered to be an accurate reflection of the molecular weight distribution of the corresponding poly(BMA-*co*-NAS-*graft*-RAFT agent). The evolution of shoulders in molecular weight distributions during the process of immobilizing RAFT agents (due to suggested molecular coupling reactions as a result of peroxides present as impurities in ether solvent acting as radical sources) have been reported elsewhere.[34] In our case the immobilization reaction was conducted in $CHCl_3$, a solvent in which a minimal amount of peroxides are expected (as opposed to an ether), thereby avoiding this problem. The orientation of the immobilized RAFT agents on the poly(BMA-*co*-NAS-*graft*-RAFT agent) were such that any propagating radical would always propagate as a growing side chain in a direction that is away from the backbone. This resulted in the trithio moiety always being situated on the chain ends of the side chains. This is beneficial as it allows subsequent removal of the trithio moieties if desired and decreasing steric hindrance around the propagating radical as the polymerization reaction proceeds.[34] This scenario also lowers the probability of homopolymer formation during branch propagation since this orientation of the RAFT agent will result in few unbound free radicals. The only mobile free radicals would be generated from the primary free radical source, short oligomeric radicals formed from the first few propagation steps before addition, and possible unwanted transfer reactions.

Poly(BMA-*co*-NAS-*graft*-BMA) Synthesis. Poly(BMA-*co*-NAS-*graft*-RAFT agent) chains with immobilized RAFT agents along the length of the polymer backbone were obtained in good yield. Upon addition of a primary free radical source and monomer, chain growth commenced from these points, resulting in comblike structures, shown in Scheme 4. The use of RAFT agents with benzyl groups as leaving groups has been reported in the literature, but in all reported cases symmetrical trithiocarbonates such as *S*,*S*′-dibenzyl trithiocarbonate were employed.[70,71] This necessarily leads to benzyl groups acting as initiating species. During branch growth from poly(BMA-*co*-NAS-*graft*-RAFT agent) described in this study, there is competition between a secondary radical (segment of immobilized RAFT agent attached to polymer backbone) and a primary radical (benzyl group) leaving. As a secondary radical is more stable than a primary radical, it would be expected that a secondary radical will preferentially act as leaving group. Any significant BMA insertion between the sulfur and benzyl group will cause the benzylic $-CH_2-$ singlet in the ^1H NMR spectrum (Figure 11) to shift upfield and increase in multiplicity. Comparison of the ^1H NMR spectra of pure (benzyl 2-(2-hydroxyethylamino)-1-methyl-2-oxoethyl trithiocarbonate (**4**) and poly(BMA-*co*-NAS-*graft*-RAFT agent) showed that the chemical shift and multiplicity of the benzylic $-CH_2-$ signal (2 H at ca. δ = 4.61 ppm, $CDCl_3$) remained unchanged. This indicates that no significant insertion of BMA units between the sulfur and benzyl group had occurred. Branch growth proceeded to high conversions: 77% and 64% for poly(BMA-*co*-NAS) containing 20% NAS and 10% NAS, respectively. The branch $\bar{M}_n$ was calculated by means of the percentage

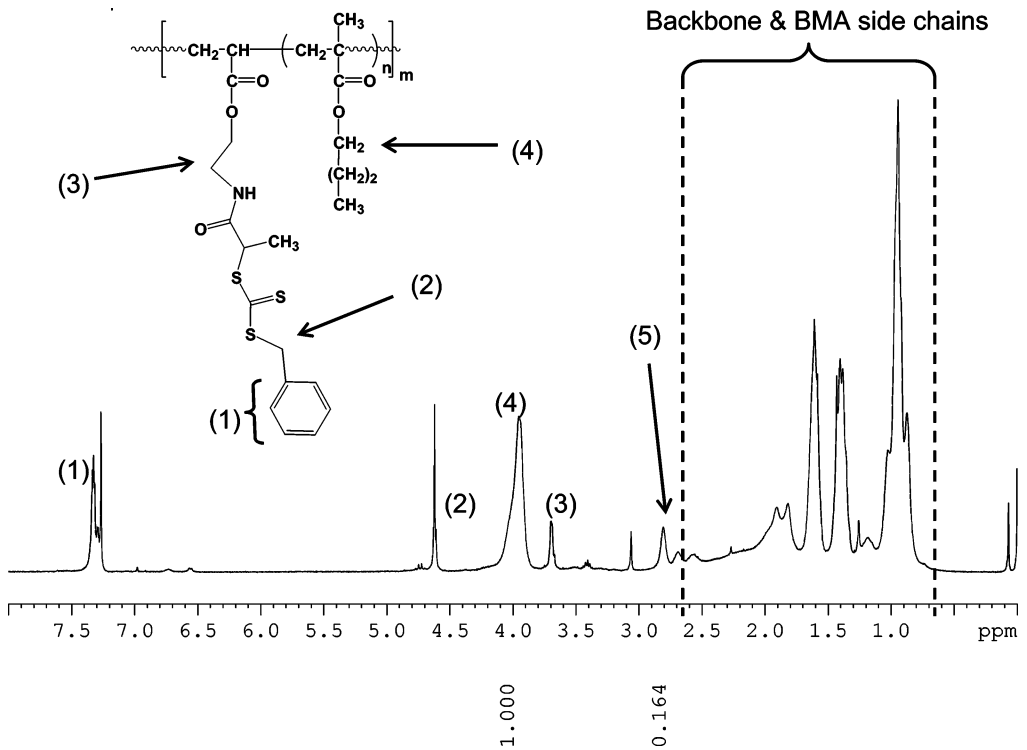

Figure 11. ^{1}H NMR spectrum of a poly(BMA-*co*-NAS) chain activated by reacting ca. 83% of the NAS units with RAFT agent (**4**). The BMA alkyl ester $-CH_2O-$ group, used as internal reference to calculate grafting yield, is shown by the peak labeled 4 and residual NAS units (not explicitly shown in accompanying figure) by the peak labeled 5. The relative integration values of peaks 4 and 5 are also shown.

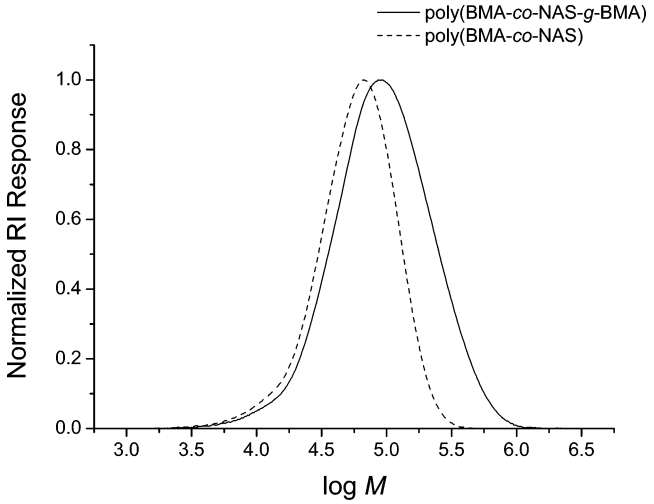

Figure 12. Comparison of the (apparent) molecular weight distributions (PSt equivalents) of poly(BMA-*co*-NAS) ($\bar{M}_n$ = 45 200, PDI = 1.67) containing 10% NAS (~50% activated) with the resulting poly(BMA-*co*-NAS-*graft*-BMA) (comb $\bar{M}_n$ = 51 900, PDI = 2.09, calculated branch $\bar{M}_n$ ~ 3800).

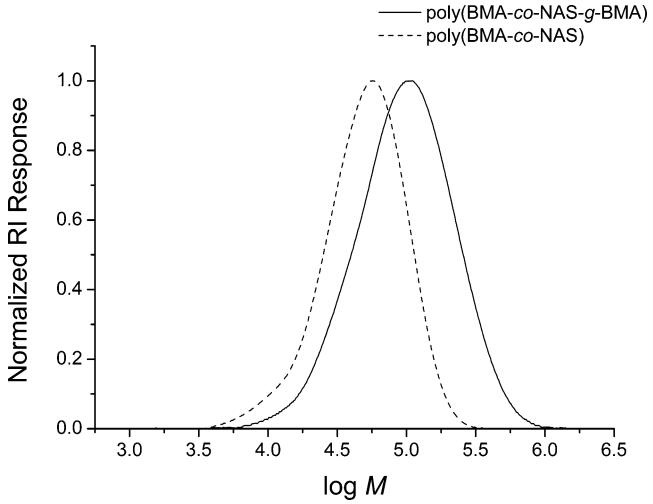

Figure 13. Comparison of the (apparent) molecular weight distributions (PSt equivalents) of poly(BMA-*co*-NAS) ($\bar{M}_n$ = 35 300, PDI = 1.65) containing 20% NAS (~83% activated) with the resulting poly(BMA-*co*-NAS-*graft*-BMA) (comb $\bar{M}_n$ = 56 200, PDI = 1.93, calculated branch $\bar{M}_n$ ~ 4700).

conversion of targeted branch $\bar{M}_n$ (6000 in this case): calculated branch $\bar{M}_n$ = (% conversion obtained during branch growth step) × 6000. SEC analysis of nonlinear polymers, including the present comb architecture, results in separation based on hydrodynamic volume, which of course is not simply related to molecular weight. With this caveat, the SEC chromatograms now discussed are presented as apparent molecular weight distributions, where it is understood that the abscissa is in fact the molecular weight of a linear polystyrene chain with the same hydrodynamic volume as that of the polymer being eluted. Figures 12 and 13 compare the molecular weight distribution for the poly(BMA-*co*-NAS) that served as backbone with the apparent molecular weight distribution of the resulting poly(BMA-*co*-NAS-*graft*-BMA). The increase in apparent molecular weight in going from linear backbone to final comblike polymer is more evident in Figure 13 than is the case in Figure 12. This could be because in the polymer in Figure 12, the linear chain containing 10% NAS was only activated to a ~50% grafting yield in terms of RAFT agent immobilization. This would lead to a much lower branch number (and subsequent molecular weight) than in the case depicted in Figure 13. No significant broadening of the apparent molecular weight distribution or secondary distributions at either lower (new,

unbound polymer chains) or higher molecular weight (coupled products) were observed, in contrast to other controlled syntheses of comb polymers reported elsewhere.[34,72,73] Significant amounts of free homopolymer formed during the synthesis of the side chains would be expected to be clearly visible as humps in the low molecular weight regions, while intra- or intermolecular cross-linking products arising from radical−radical coupling between propagating branches would be expected to be shown in the form of humps or shoulders in the high molecular weight regions. The data in Figures 12 and 13 suggest that the formation of free homopolymer in the second-stage polymerization was largely circumvented and that significant intra- or intermolecular cross-linking was largely avoided. Even though the comb branches could not be cleaved off and characterized separately, Figures 12 and 13 show that the resulting apparent molecular weight distributions remained relatively narrow and monomodal. This supports the supposition that the comb polymers have well-controlled molecular weight of the branches: comb polymers composed of branches where the branches exhibited a broad molecular weight distribution would show broader global apparent molecular weight distributions than the parent polymer, due to the major differences in subsequent hydrodynamic volumes.[34] The supposition that the branch polydispersities are low is supported by the data for BMA homopolymers in Figure 10. The narrow polydispersities of those polymers, synthesized with similar trithiocarbonate RAFT agents under similar conditions, imply that the branch chains would exhibit similar (low) polydispersity.

Conclusions

Terminal-model reactivity ratios in the conventional free radical copolymerization of BMA and NAS were determined by monitoring the decrease in individual free monomer concentrations using ^{1}H NMR spectrometry. A simple least-squares nonlinear fit procedure to the copolymer equation (eq 1) was used to determine the values of the reactivity ratios. Initial rough estimates of the values of the reactivity ratios were determined after which the Tidwell−Mortimer method was employed to refine the values. The final values of the reactivity ratios were calculated as $r_{BMA} = 0.24$ (+0.089, −0.060) and $r_{NAS} = 0.22$ (+0.037, −0.024); the numbers in parentheses represent the extremes of the joint confidence interval for these reactivity ratios, given in Figure 3. These reactivity ratios suggest that, with a slight drift with feed composition, BMA/NAS copolymer composition should remain relatively close to the azeotrope, implying that the distribution of branch points in the final comb polymer should be random.

Copolymers of BMA and NAS were polymerized by RAFT-mediated free radical polymerization, resulting in a main backbone showing controlled molecular weight distribution, while the distribution of NAS functionality along the backbone should be random. The immobilization of the primary hydroxy-functionalized RAFT agents onto the poly(BMA-*co*-NAS) backbone took place through substitution reactions of the primary hydroxy functionalities with the activated ester groups. The presence of the immobilized RAFT agents on the poly(BMA-*co*-NAS) backbone was shown by ^{1}H NMR spectrometry. The growing of side chains in the synthesis of poly(BMA-*co*-NAS-*graft*-BMA) proceeded to high conversions. The molecular weight distribution profiles of backbone poly(BMA-*co*-NAS), and the distribution of the resulting poly(BMA-*co*-NAS-*graft*-BMA) in terms of equivalent hydrodynamic volume, were similar, with no significant broadening occurring. This is consistent with the supposition that homopolymer formation and molecular cross-linking were minimized during the second stage polymerization. This suggests that the procedure used here results in comb polymers whose backbone and branch molecular weight distributions are well controlled and that the distribution of branch points is random.

Acknowledgment. The support of an ARC Discovery grant is gratefully acknowledged. Dr. Simone Vonwiller kindly synthesized the benzyl 2-(2-hydroxyethylamino)-1-methyl-2-oxoethyl trithiocarbonate and gave highly appreciated assistance with other synthetic procedures. Dr. Ian Luck kindly provided assistance with NMR spectrometer operation and analyses. Dulux Australia is gratefully acknowledged for the supply of 2-{[(dodecylsulfanyl)carbonothioyl]sulfanyl}propanoic acid. The Key Centre for Polymer Colloids is established and supported under the Australian Research Council's Research Centres Program.

References and Notes

(1) Former, C.; Castro, J.; Fellows, C. M.; Tanner, R. I.; Gilbert, R. G. *J. Polym. Sci., Polym. Chem.* **2002**, *40*, 3335−3349.
(2) Gownder, M. *J. Plast. Film Sheeting* **2001**, *17*, 53−61.
(3) Romm, F.; Figovsky, O. *Macromol. Theory Simul.* **2002**, *11*, 93−101.
(4) Xu, X. R.; Xu, J. T.; Feng, L. X.; Chen, W. *J. Appl. Polym. Sci.* **2000**, *77*, 1709−1715.
(5) Yan, D.; Wang, W. J.; Zhu, S. *Polymer* **1999**, *40*, 1737−1744.
(6) Niimi, L.; Serita, K.; Hiraoka, S.; Yokozawa, T. *J. Polym. Sci., Polym. Chem.* **2002**, *40*, 1236−1242.
(7) Brenner, A. R.; Schmaljohann, D.; Voit, B. I.; Wolf, D. *Macromol. Symp.* **1997**, *122*, 217−222.
(8) Hadjichristidis, N.; Xenidou, M.; Iatrou, H.; Pitsikalis, M.; Poulos, Y.; Avgeropoulos, A.; Sioula, S.; Paraskeva, S.; Velis, G.; Lohse, D. J.; Schulz, D. N.; Fetters, L. J.; Wright, P. J.; Mendelson, R. A.; García-Franco, C. A.; Sun, T.; Ruff, C. J. *Macromolecules* **2000**, *33*, 2424−2436.
(9) Pi, Z.; Kennedy, J. P.; Summers, J. W. *J. Polym. Sci., Polym. Chem.* **2002**, *40*, 3644−3651.
(10) Hirao, A.; Kawano, H.; Ryu, S. W. *Polym. Adv. Technol.* **2002**, *13*, 275−284.
(11) Hua, F. J.; Liu, B.; Hu, C. P.; Yang, Y. L. *J. Polym. Sci., Polym. Chem.* **2002**, *40*, 1876−1884.
(12) Chiefari, J.; Chong, Y. K.; Ercole, F.; Krstina, J.; Jeffery, J.; Le, T. P. T.; Mayadunne, R. T. A.; Meijs, G. F.; Moad, C. L.; Moad, G.; Rizzardo, E.; Thang, S. H. *Macromolecules* **1998**, *31*, 5559−5562.
(13) Wang, J.; Matyjaszewski, K. *J. Am. Chem. Soc.* **1995**, *117*, 5614−5615.
(14) Georges, M. K.; Hamer, G. K.; Listigovers, N. A. *Macromolecules* **1998**, *31*, 9087−9089.
(15) Haddleton, D. M.; Maloney, D. R.; Suddaby, K. G. *Macromolecules* **1996**, *29*, 481−483.
(16) Haddleton, D. M.; Maloney, D. R.; Suddaby, K. G.; Clarke, A.; Richards, S. N. *Polymer* **1997**, *38*, 6207−6217.
(17) Kukulj, D.; Heuts, J. P. A.; Davis, T. P. *Macromolecules* **1998**, *31*, 6034−6041.
(18) Berlinova, I. V.; Dimitrov, I. V.; Vladimirov, N. G.; Samichkov, V.; Ivanov, Y. *Polymer* **2001**, *42*, 5963−5971.
(19) Börner, H. G.; Matyjaszewski, K. *Macromol. Symp.* **2002**, *177*, 1−15.
(20) Bon, S. A. F.; Morsley, D. R.; Waterson, C.; Haddleton, D. M. *Macromolecules* **2000**, *33*, 5819−5824.
(21) Chiefari, J.; Jeffery, J.; Mayadunne, R.; Moad, G.; Rizzardo, E.; Thang, S. *Macromolecules* **1999**, *32*, 7700−7702.
(22) Mecerreyes, D.; Pomposo, J. A.; Bengoetxea, M.; Grande, H. *Macromolecules* **2000**, *33*, 5846−5849.
(23) Zeng, F.; Shen, Y.; Zhu, S.; Pelton, R. *Macromolecules* **2000**, *33*, 1628−1635.
(24) Coessens, V.; Pintauer, T.; Matyjaszewski, K. *Prog. Polym. Sci.* **2001**, *26*, 337−377.

(25) Matyjaszewski, K.; Beers, K. L.; Kern, A.; Gaynor, S. G. *J. Polym. Sci., Polym. Chem.* **1998**, *36*, 823−830.
(26) Roos, S. G.; Müller, A. H. E.; Matyjaszewski, K. *Macromolecules* **1999**, *32*, 8331−8335.
(27) Cacioli, P.; Hawthorne, D. G.; Laslett, R. L.; Rizzardo, E.; Solomon, D. H. *J. Macrom. Sci., Chem.* **1986**, *A23*, 839−852.
(28) Sprong, E.; De Wet-Roos, D.; Tonge, M.; Sanderson, R. D. *J. Polym. Sci., Polym. Chem.* **2003**, *41*, 223−235.
(29) Penn, L. S.; Hunter, T. F.; Lee, Y.; Quirk, R. P. *Macromolecules* **2000**, *33*, 1105−1107.
(30) Hou, S.; Kuo, P. *Polymer* **2001**, *42*, 2387−2394.
(31) Tong, J.-D.; Du Prez, F. E.; Goethals, E. J. *Macromolecules* **2001**, *34*, 761−767.
(32) (a) D'Agosto, F.; Charreyre, M.-T.; Mélis, F.; Mandrand, B.; Pichot, C. *J. Appl. Polym. Sci.* **2003**, *88*, 1808−1816. (b) Charreyre, M.-T.; D'Agosto, F.; Favier, A.; Pichot, C.; Mandrand, B. Biocompatible polymers for fixing biological ligands, WO 092361, 2001.
(33) Li, Z.; Du, Q. G.; Yang, Y. L.; Lin, M. D. *Macromol. Chem. Phys.* **2001**, *202*, 2314−2320.
(34) Quinn, J. F.; Chaplin, R. P.; Davis, T. P. *J. Polym. Sci., Polym. Chem.* **2002**, *40*, 2956−2966.
(35) Guo, X. P.; Li, Z. A.; Du, Q. G.; Yang, Y. L.; Lin, M. D. *J. Appl. Polym. Sci.* **2002**, *84*, 2318−2326.
(36) Martínez, G.; de Santos, E.; Millán, J. L. *Macromol. Chem. Phys.* **2001**, *202*, 2377−2386.
(37) Börner, H. G.; Beers, K. L.; Matyjaszewski, K.; Sheiko, S. S.; Möller, M. *Macromolecules* **2001**, *34*, 4375−4383.
(38) Lee, A. H. F.; Chan, A. S. C.; Li, T. H. *Tetrahedron* **2003**, *59*, 833−839.
(39) Lewis, M. R.; Boswell, C. A.; Laforest, R.; Buettner, T. L.; Ye, D.; Connett, J. M.; Anderson, C. J. *Cancer Biother. Radiopharm.* **2001**, *16*, 483−494.
(40) Loiseau, N.; Cavelier, F.; Noel, J. P.; Gomis, J. M. *J. Pept. Sci.* **2002**, *8*, 335−346.
(41) Luo, Y.; Prestwich, G. D. *Bioconjugate Chem.* **2001**, *12*, 1085−1088.
(42) Takei, Y. G.; Matsukata, M.; Aoki, T.; Sanui, K.; Ogata, N.; Kikuchi, A.; Sakurai, Y.; Okano, T. *Bioconjugate Chem.* **1994**, *5*, 577−582.
(43) Zhang, H. T.; Guo, Z. R.; Huang, J. L. *J. Polym. Sci., Polym. Chem.* **2002**, *40*, 4398−4403.
(44) D'Agosto, F.; Charreyre, M.-T.; Veron, L.; Llauro, M.-F.; Pichot, C. *Macromol. Chem. Phys.* **2001**, *202*, 1689−1699.
(45) Erout, M. N.; Elaïssari, A.; Pichot, C.; Llauro, M.-F. *Polymer* **1996**, *37*, 1157−1165.
(46) Erout, M. N.; Troesch, A.; Pichot, C.; Cros, P. *Bioconjugate Chem.* **1996**, *7*, 568−575.
(47) Yang, H. J.; Cole, C. A.; Monji, N.; Hoffman, A. S. *J. Polym. Sci., Polym. Chem.* **1990**, *28*, 219−226.
(48) Yoshida, M.; Asano, M.; Yokota, T.; Chosdu, R.; Kumakura, M. *J. Polym. Sci., Polym. Lett.* **1989**, *27*, 437−442.
(49) Yoshida, M.; Asano, M.; Yokota, T.; Kumakura, M. *Polymer* **1990**, *31*, 371−378.
(50) Monji, N.; Cole, C. A.; Hoffman, A. S. *J. Biomater. Sci., Polym. Ed.* **1994**, *5*, 407−420.
(51) Cole, C. A.; Schreiner, S. M.; Priest, J. H.; Monji, N.; Hoffman, A. S. *ACS Symp. Ser.* **1987**, *350*, 245−254.
(52) Chen, J. P.; Chiu, S. H. *Enzyme Microb. Technol.* **2000**, *26*, 359−367.
(53) Mayo, F. R.; Lewis, F. M. *J. Am. Chem. Soc.* **1944**, *66*, 1594−1601.
(54) Stevens, M. P. *Polymer Chemistry−An Introduction*, 3rd ed.; Oxford University Press: Oxford, 1999.
(55) O'Driscoll, K. F.; Reilly, P. M. *Makromol. Chem., Macromol. Symp.* **1987**, *10/11*, 355−374.
(56) Moineau, G.; Minet, M.; Dubois, P.; Teyssié, P.; Senninger, T.; Jérôme, R. *Macromolecules* **1999**, *32*, 27−35.
(57) Matyjaszewski, K. *Macromolecules* **1998**, *31*, 4710−4717.
(58) Arehart, S. V.; Matyjaszewski, K. *Macromolecules* **1999**, *32*, 2221−2231.
(59) Hawthorne, D. G.; Moad, G.; Rizzardo, E.; Thang, S. H. *Macromolecules* **1999**, *32*, 5457−5459.
(60) Calitz, F. M.; Tonge, M. P.; Sanderson, R. D. *Macromolecules* **2003**, *36*, 5−8.
(61) Ferguson, C. J.; Hughes, R. J.; Pham, B. T. T.; Hawkett, B. S.; Gilbert, R. G.; Serelis, A. K.; Such, C. H. *Macromolecules* **2002**, *35*, 9243−9245.
(62) D'Agosto, F.; Charreyre, M.-T.; Pichot, C. *Macromol. Biosci.* **2001**, *1*, 322−328.
(63) Braun, S.; Kalinowski, H.-O.; Berger, S. *150 and More Basic NMR Experiments*; Wiley-VCH: Weinheim, 1998.
(64) Van Herk, A. *J. Chem. Educ.* **1995**, *72*, 138−140.
(65) Tidwell, P. W.; Mortimer, G. A. *J. Polym. Sci., Polym. Chem.* **1965**, *3*, 369−387.
(66) Brar, A. S.; Kumar, R. *J. Mol. Struct.* **2002**, *616*, 37−47.
(67) Ito, H.; Dalby, C.; Pomerantz, A.; Sherwood, M.; Sato, R.; Sooriyakumaran, R.; Guy, K.; Breyta, G. *Macromolecules* **2000**, *33*, 5080−5089.
(68) O'Driscoll, K. F. *J. Macrom. Sci., Chem.* **1969**, *A3*, 307−309.
(69) Lai, J. T.; Filla, D.; Shea, R. *Macromolecules* **2002**, *35*, 6754−6756.
(70) Mayadunne, R. T. A.; Rizzardo, E.; Chiefari, J.; Krstina, J.; Moad, G.; Postma, A.; Thang, S. H. *Macromolecules* **2000**, *33*, 243−245.
(71) Quinn, J. F.; Barner, L.; Davis, T. P.; Thang, S. H.; Rizzardo, E. *Macromol. Rapid Commun.* **2002**, *23*, 717−721.
(72) Fernández-García, M.; De la Fuente, J. L.; Cerrada, M. L.; Madruga, E. L. *Polymer* **2002**, *43*, 3173−3179.
(73) Wang, Z.; He, J.; Tao, Y.; Yang, L.; Jiang, H.; Yang, Y. *Macromolecules* **2003**, *36*, 7446−7452.

MA035302A